UPPSALA
UNIVERSITET

Digital Comprehensive Summaries of Uppsala Dissertations from the Faculty of Science and Technology 933

Advanced MEMS Pressure Sensors Operating in Fluids

EMIL ANDERÅS

ACTA
UNIVERSITATIS
UPSALIENSIS
UPPSALA
2012

ISSN 1651-6214
ISBN 978-91-554-8369-2
urn:nbn:se:uu:diva-173182

Dissertation presented at Uppsala University to be publicly examined in Polhelmsalen, Ångströmslaboratoriet, Lägerhyddsvägen 1, Uppsala, Tuesday, June 5, 2012 at 10:00 for the degree of Doctor of Philosophy. The examination will be conducted in English.

Abstract
Anderås, E. 2012. Advanced MEMS Pressure Sensors Operating in Fluids. Acta Universitatis Upsaliensis. *Digital Comprehensive Summaries of Uppsala Dissertations from the Faculty of Science and Technology* 933. 54 pp. Uppsala. ISBN 978-91-554-8369-2.

Today's MEMS technology allows manufacturing of miniaturized, low power sensors that sometimes exceeds the performance of conventional sensors. The pressure sensor market today is dominated by MEMS pressure sensors.

In this thesis two different pressure sensor techniques are studied. The first concerns ways to improve the sensitivity in the most commonly occurring pressure sensor, namely such based on the piezoresistive technique. Since the giant piezoresistive effect was observed in silicon nanowires, it was assumed that a similar effect could be expected in nano-thin silicon films. However, it turned out that the conductivity was extremely sensitive to substrate bias and could therefore be controlled by varying the backside potential. Another important parameter was the resistivity time drift. Long time measurements showed a drastic variation in the resistance. Not even after several hours of measurement was steady state reached. The drift is explained by hole injection into the buried oxide as well as existence of mobile charges. The piezoresistive effect was studied and shown to be of the same magnitude as in bulk silicon. Later research has shown the existence of such an effect where the film thickness has to be less than around 20 nm.

The second area that has been studied is the pressure sensitivity of in acoustic resonators. Aluminium nitride thin film plate acoustic resonators (FPAR) operating at the lowest-order symmetric (S0), the first-order asymmetric (A1) as well as the first-order symmetric (S1) Lamb modes have been theoretically and experimentally studied in a comparative manner. The S0 Lamb mode is identified as the most pressure sensitive FPAR mode. The theoretical predictions were found to be in good agreement with the experiments. Additionally, the Lamb modes have been tested for their sensitivities to mass loading and their ability to operate in liquids, where the S0 mode showed good results.

Finally, the pressure sensitivity in aluminium nitride thin film bulk wave resonators employing c- and tilted c-axis texture has been studied. The c-axis tilted FBAR demonstrates a substantially higher pressure sensitivity compared to its c-axis oriented counterpart.

Keywords: pressure sensor, piezoresistance, nanofilms, AlN, microacoustic, Lamb wave, thin film, resonator, sensitivity

Emil Anderås, Uppsala University, Department of Engineering Sciences, Solid State Electronics, Box 534, SE-751 21 Uppsala, Sweden.

ISSN 1651-6214
ISBN 978-91-554-8369-2
urn:nbn:se:uu:diva-173182 (http://urn.kb.se/resolve?urn=urn:nbn:se:uu:diva-173182)

1 Kor 1:19

List of Papers

This thesis is based on the following papers, which are referred to in the text by their Roman numerals.

I Anderås, E., Vestling, L., Olsson, J., Katardjiev, I., (2009) Resistance Electric Field Dependence and Time Drift of Piezoresistive Single Crystalline Silicon Nanofilms *Procedia Chemistry*, *Proceedings of the Eurosensors XXIII,* 1(1):80–83

II Anderås, E., Vallin, Ö., Vestling, L., Katardjiev, I., Olsson, J., (2010) Drift in Thin Film SOI Piezoresistors *Proceedings of EUROSOI Workshop,* 1(1):71–72

III Arapan, L., Anderås, E., Katardjiev, I., Yantchev, V., (2011) Sensitivity Features of Thin Film Plate Acoustic Wave Resonators *IEEE sensors journal,* 11(12):3330–3331

IV Anderås, E., Katardjiev, I., Yantchev, V., (2011) Lamb wave resonant pressure micro-sensor utilizing a thin film aluminium nitride membrane *Journal of Micromechanics and Microengineering,* 21(8):085010

V Anderås, E., Arapan, L., Katardjiev, I., Yantchev, V., (2011) Thin Film Plate Wave Resonant Sensor for Pressure and Gravimetric Measurements *Procedia Engineering, Eurosensors XXV,* 1(1):71–72

VI Anderås, E., Katardjiev, I., Yantchev, V., (2012) Tilted c-axis Thin-Film Bulk Wave Resonant Pressure Sensors with Improved Sensitivity *IEEE sensors journal*

Contents

Abbreviations

BAW	Bulk Acoustic Wave Resonator
FBAR	Thin Film Bulk Acoustic Wave Resonator
FEM	Finite Element Method
FPAR	Thin Film Plate Acoustic Wave Resonator
GPR	Giant Piezoresistance
HF	Hydrofluoric acid
IDT	Interdigital Transducer
MEMS	Microelectromechanical Systems
QCM	Quartz Crystal Microbalance
SAW	Surface Acoustic Wave
SMR	Solidly Mounted Resonator
SNR	Signal to Noise Ratio
SOI	Silicon On Insulator
TCAD	Transactions on Computer-Aided Design
TCR	Temperature Coefficient of Resistivity
TEA	Thin Film Electroacoustic
TMAH	Tetramethylammonium Hydroxide

1 Introduction

”Pressure sensor: an instrument component that detects a fluid pressure and produces an electrical signal related to the pressure.”

Microelectromechanical systems (MEMS) have been a topic of substantial interest in recent years due to their great potential to make miniaturized devices at a low cost and low power consumption while often exhibiting higher performance than conventional counterparts. MEMS pressure sensors currently dominate the market for pressures greater than atmospheric pressure. The largest area for MEMS pressure sensors is the automotive industry where the sensors operate in harsh environments monitoring the tire pressure or in automatic transmission etc. The second largest area is medical electronics such as low-cost disposable in vivo pressure sensors, or pressure and differential flow monitoring in machines for treating sleep apnea, etc. They can also be found in household machines such as dishwashers, washing machines and vacuum cleaners. It is also said that the MEMS pressure sensor will be the next integrated component (altimeters) in smartphones and tablet PCs and therefore they are predicted to be the leading MEMS device by 2014 [1].

The MEMS pressure sensors are almost exclusively diaphragm-based devices where the diaphragm deflects due to an applied pressure differential. There are several ways to measure the deflection but the two most frequently used are the piezoresistive and the capacitive approaches respectively. The former uses the piezoresistive effect in silicon resistors which are fabricated in or on the deflecting diaphragm while the latter senses the capacitive change due to the change in distance between two plates. These sensors are easily manufactured using the well established surface and bulk micromachining techniques.

Other interesting MEMS based pressure sensitive configurations are acoustic wave sensors. As an acoustic wave propagates through or on the surface of the material, any perturbations along the propagation path (the membrane in this case) affect the velocity and/or amplitude of the wave. By way of example, a deformation of the membrane would induce stress in the latter resulting in a perturbation in the stiffness constants, and hence, in the wave velocity. These variations can be monitored by measuring the frequency characteristics of the sensor where a frequency shift in the above context is related to a change in the ambient pressure. Two of the most

common types of acoustic devices are quartz crystal microbalance (QCM) and surface acoustic wave (SAW) components (resonators, filters, etc). They make use of single crystalline materials such as quartz, $LiNbO_3$, $LiTaO_3$, etc. Since a pressure sensor is a device where applied pressure causes a measurable deformation, these devices would not be suitable except for very high pressure applications. However, with the recently developed thin film piezoelectric technology, membrane based acoustic resonators with a large area to thickness ratio have become feasible. These devices have shown excellent acoustic properties, such as high Q and low noise. The large aspect ratio is expected to result in high pressure sensitivity which combined with the excellent acoustic properties of the thin piezoelectric films should yield, high resolution pressure sensors. Other advantages of such devices are that they are passive and can be interrogated wirelessly, which makes them suitable for inaccessible locations or on rotating parts for example in car tires. The sensors can also be used in hazardous environments such as contaminated, high voltages or radioactive areas, where the use of conventional pressure sensors is complicated.

Pressure sensors are often classified in terms of in what pressure or temperature range they operate or in what type of pressure they measure, though the same technology may be used in different classes. Since MEMS pressure sensors most often are membrane based, they are used as differential pressure sensors, i.e., they measure the difference between two pressures. The ranges the sensors operate in can therefore vary drastically. The maximum pressure difference they can handle depends on the material and the aspect ratio of the membrane. The pressure sensors used in this thesis was tested up to 160 kPa.

This thesis deals with the design, fabrication and evaluation of two types of MEMS pressure sensors based on the piezoresistive and piezorelectric approaches respectively. Thus, it can be divided into two parts. The focus of the first part is the piezoresistive pressure sensor. The piezoresistive approach is the most common among MEMS pressure sensors. The sensors are often manufactured using well established processes of surface micromachining where polycrystalline silicon, also called polysilicon, is used as the piezoresistive element instead of single-crystalline silicon. The piezoresistive effect in polysilicon is approximately 6 – 7 times smaller than that of single-crystalline silicon. This means that the sensitivity of these sensors is relatively low. Here a method to increase the piezoresistive effect in silicon has been investigated and presented

The second part of this thesis deals with a new class of sensors, namely pressure sensors employing acoustic wave resonators where two specific types have been thoroughly investigated - thin film plate acoustic wave resonators (FPAR) and thin film bulk acoustic wave resonators (FBAR).

1.2 Pressure fundamentals

A closed vessel contains a large number of atoms and molecules that are constantly moving and bouncing off its walls. The pressure would be the average force that these atoms and molecules exert per unit area on the walls of the vessel. The definition of pressure is therefore defined as force per unit area that a fluid exerts on its surroundings. Pressure can also be measured as a function of the weight of the fluid above it. The pressure at a given point therefore depends on the height of a fluid above that point, the density of the fluid and the gravitational field. Though sometimes other factors must be taken into consideration e.g. when the atmospheric pressure is measured, the fact that the density of air varies along the Earth's gravitational field makes the calculations more complicated.

During time many different units for pressure have been used. The SI unit for pressure is by the definition Pascal (N/m^2). Though, many different units are used for different applications. Other familiar units of pressure are bar, atmosphere and millimeter of mercury. Throughout this thesis the SI unit Pascal will be used.

1.3 Sensitivity and resolution

The two most important properties of a sensor are the sensitivity and the resolution. From the academic point of view, the sensitivity is often considered as more important, whereas in industrial applications, the resolution is of greater practical use. However, these two concepts are often easily confused by the general reader. The general definition for sensitivity is:

> **Sensitivity (S):** The ratio between the output signal and the measured property variations.

That is, the sensitivity is a measure of the sensor's output variations as a function of the measurand variations. For example in a piezoresistive pressure sensor, the sensitivity represents the resistance variation for a given pressure variation, i.e. dR/dP. However, the term 'sensitivity' is often used in the same manner as what in the sensor science is referred to as:

> **Resolution (R):** The smallest detectable change of the measurand.

The resolution is defined as the ratio between three times the smallest detectable signal (σ) and the sensitivity:

$$R = {}^{3\sigma}/_{S} \tag{1}$$

The smallest detectable signal is limited by the overall noise in the measurement. That could be variations in ambient factors such as temperature, pressure and electrical fields or internal noise within the sensor such as thermal and electrical vibrations. In most sensor applications the ‘resolution’ is the property of interest.

2 Piezoresistive pressure sensor

2.1 Theory

The piezoresistive effect of silicon was discovered in the 1950s and since then silicon-based pressure sensors have been developed and commercially manufactured. A typical piezoresistive pressure sensor is a thin circular or rectangular membrane where the deflection due to applied external pressure is measured indirectly. The membranes can be made from the same material as the wafer substrate, usually silicon or from thin films e.g. silicon oxide, polysilicon, nitride etc.[2] The piezoresistive elements may be integrated resistors which are doped areas made through diffusion, ion implantation or doped epitaxy. However, these PN junction isolated piezoresistors become leaky, especially at temperatures above 100 °C. One way to overcome this problem is by fabricate the pressure sensors on silicon-on-insulator (SOI) substrates where the resistors are insulated by silicon oxide [3]. Another method is to make the piezoresistors out of polysilicon which involves inexpensive, easy and standard planar processes and has the advantage that the temperature coefficient of resistivity (TCR) can be chosen or be made zero by suitably adjusting the doping concentration [4]. Other advantages with the polysilicon based sensors are that they can work in high temperature environments, the required die size can be decreased and the integration with electronics is simplified. However, notable drawbacks include a reduced pressure sensitivity since the gauge factor of polysilicon is six to seven times lower than that of single crystalline silicon [4] and poor reproducibility of mechanical properties. When the membranes deflect due to applied pressure, the maximum strain occurs at the edges of the membrane. The piezoresistors are therefore located near the membrane edges to attain maximum sensitivity, see *Figure 1a*.

The resistance changes are often measured using a Wheatstone bridge circuit configuration. It consists of four resistors connected in a loop, see *Figure 1b*. Often, it is only one of the resistors that changes its resistance due to membrane deflection while the others are made insensitive to strain. This provides an output voltage proportional to the resistance change. This setup offers an increased sensitivity and a correction for zero shift with temperature.

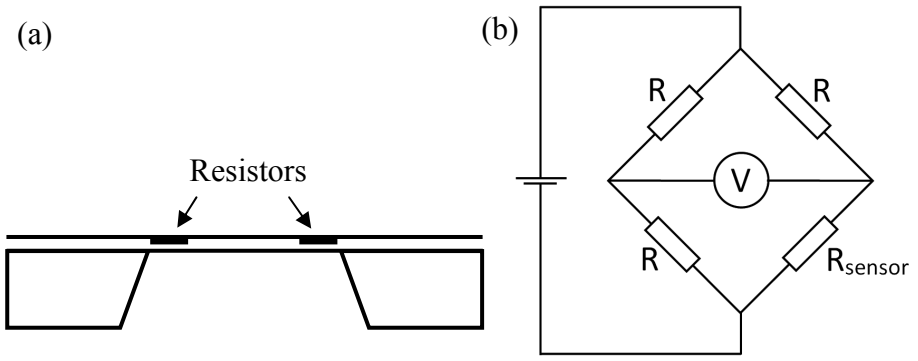

Figure 1. (a) A membrane with resistors (b) Wheatstone bridge configuration

2.1.1 Piezoresistivity

The resistance of a resistor is given by:

$$R = \rho \frac{l}{A} \tag{2}$$

where ρ is the resistivity, l is the length and A is the cross-sectional area. When a resistor is strained, the length and the area changes following Poisson's ratio and the resistance changes accordingly. This phenomenon is sometimes included in the term piezoresistance even though by strict definition, piezoresistance refers to the phenomenon where the *resistivity* changes due to applied stress. Metal resistors for example, change their resistance under strain due to shape deformation and are called strain gauges, however in silicon resistors the resistivity changes due to stress and are therefore true piezoresistors.

$$\rho = \frac{1}{q\mu_n n + q\mu_p p} \tag{3}$$

In a semiconductor the resistivity depends on the mobility and the concentration of the charge carriers according to (3). The mobility depends on both the mean free path between carrier collisions and the effective mass of the carrier in the crystal lattice, both of which change under applied stress or deformation. The quantum-physical explanation of the piezoresistive effect is further explained in reference [5].

The change in resistivity due to stress is described by the Piezoresistivity coefficient π and is defined as the fractional change in resistivity per unit stress:

$$\pi = \frac{\Delta\rho/\rho}{T} \tag{4}$$

where T is stress. In anisotropic material such as silicon, the piezoresistive coefficients depend on the crystalline orientation and direction of the current with respect to stress.

2.2 Sensitivity improvements

As mentioned above, the piezoresistive element in pressure sensors is often made of polysilicon. However, the sensitivity of the polysilicon resistors may not be sufficient, so instead of making single crystalline silicon resistors in the membrane through diffusion or ion implantation, attempts to bond resistors directly onto the membrane have been made, without satisfactory results [6, 7]. A number of alternative ways of improving the sensitivity in silicon have been suggested. Below a few of them are briefly presented.

2.2.1 Bottom-up silicon nanowires

A chemical vapor deposition process was used by He and Yang [8] to grow suspended nanowires in the <111> direction, with a diameter in the range 50 nm to 350 nm. The resistance was then measured under strain yielding remarkable results. The longitudinal piezoresistance coefficient was reported to be as high as -3,550 x 10^{-11} Pa^{-1}, which is almost 38 times higher than that of the bulk silicon value of -94 x 10^{-11} Pa^{-1}. This effect has been called the giant piezoresistance (GPR) effect and was found to increase when decreasing the diameter and/or when increasing the resistivity of the nanowires. In this regard the silicon nanowires are ideal as piezoresistive elements. However, this fabrication approach is not part of standard industrial processes and due to the high production cost it is not suitable for mass production.

The authors do not propose any explanation for the notable behavior of the nanowires and suggest that further theoretical work has to be done.

2.2.2 Top-down silicon nanowires

Another approach for fabricating silicon nanowires is the so called top-down method where conventional MEMS processes are used. Reck et al [9] manufactured nanowires out of a thin silicon layer on a silicon-on-insulator (SOI) wafer using an e-beam lithography for mask generation and a subsequent anisotropic reactive ion etch process for defining the nanowires in the device layer. In a similar fashion polysilicon nanowires were also made. The piezoresistive effect was measured by applying stress and simultaneously measuring the resistivity in the nanowires. In the experiment 4-point measurements were performed which method obviously could not be done in the case of free suspended nanowires. The largest measured increase in the piezoresistive effect was more the 7 times compared to that of the bulk silicon

reference. The dimensions of the nanowires were 140x200nm^2. The polysilicon nanowires showed an increase in the piezoresistive effect as well. The increase was measured to up to 34%, compared to the polysilicon reference resistor.

It is hard to compare the two different nanowires types, due to the different dimensions, crystal orientation and manufacturing process. However, the large difference in piezoresistive effect between the free suspending grown nanowires and the etched nanowires is difficult to explain. The difference in thickness uniformity between the etched and the grown nanowires as well as the fact that they are either freely suspended or lying on a substrate probably play significant roles.

2.2.3 Suggested explanation

According to *Rowe* [10] the explanation of the GPR effect is a phenomenon that had already been known in 1874 by Ferdinand Braun, but its effect is insignificantly small in ordinary MEMS electronics. However, dealing with nanoscale structures, effects that otherwise are negligible, become significant and need to be taken into consideration, which Rowe believes is the case here. The phenomenon in question is the so called pinch-off effect, which means that the surface depletion region is modulated due to stress. The density of the surface charge carriers decreases or is "pinched-off" with tensile stress. Under normal circumstances where the surface to volume ratio is very small, this effect can be neglected, but in nanowires where this ratio increases dramatically, this effect must be taken into account. According to Rowe, this is the explanation of the GPR effect measured by He and Yang. In the case of a very small nanowire where the surface area dominates over the bulk volume, the conductivity decreases dramatically due to depletion of charge carriers under tensile stress. Piezoresistivity is often explained by mobility changes due to stress, which is not the case with the GPR effect, though these two effects reinforce each other.

It is reasonable to believe that surface effects may be the explanation for the GPR effect since the surface to volume ratio is the main difference between nano-size silicon and ordinary bulk silicon, however, one must dig deeper into the subject to fully grasp the physics behind this phenomenon.

2.3 Thin silicon films

[Paper I – II]

Since the GPR effect has been observed in one dimensional resistors (nanowires) and is strongly associated with the surface to volume ratio, a similar effect is expected to be observed in two dimensional structures (nan-

ofilms) as well, admittedly with a lower magnitude due to reduced surface area to volume ratio. This section describes the work done in this thesis regarding the piezoresistive effect in thin silicon films and includes results from Papers I – II.

2.3.1 Fabrication

Since the highest piezoresistive effect is obtained with p-doped [11] single crystalline silicon, boron was implanted into SOI wafers in this experiment. Further, in nanowires the GPR effect increases with decreasing resistivity and therefore a moderate doping level was chosen. The resistivity in the SOI device layer was anticipated to be around 0.2 – 0.3 Ωcm, but ended up being around ten times that value, probably due to boron loss into the buried oxide during annealing. The aim was to obtain resistors with a resistance of about 1 MΩ. Resistors in commercial MEMS pressure sensors have a resistance of about 1 kΩ.

Etching of silicon

There are several ways to make silicon films thinner. The easiest and most controllable way is to thermally oxidize the silicon and subsequently etch away the silicon dioxide with HF. The problem with this method is that the dopants diffuse into the oxide during the oxidation process and consequently the resistivity of the silicon decreases uncontrollably. Therefore, a direct etching of silicon TMAH (tetramethylammonium hydroxide) was used here. The advantage with TMAH is that the etch rate depends on its concentration and temperature. Thus, the etch rate can be adjusted and controlled at will in view of obtaining a highly reproducible etch process. The etch rate for silicon dioxide is very low and can therefore be used as mask.

Test structures

To study the piezoresistive effect in thin films, the resistivity must be measured in a reliable way. A common method for resistivity measurements is to use a four point probe [12]. However, in the case of a very thin and highly resistive film, getting repeatable results could be difficult. Since the film is very thin, the sharp probes easily penetrate it and a stable ohmic contact is not formed. Therefore isolated strips with varying lengths and widths, with four point resistance measurement configurations [12] and with ohmic contacts had to be used to get reliable results, see *Figure 2*.

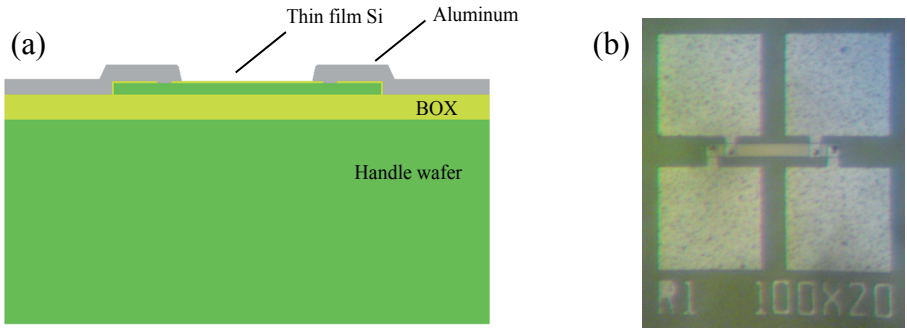

Figure 2. (a) Schematic cross-section of the test structure (b) Thin silicon film resistor with a four point resistance measurement configuration

Applying stress

If the substrates with the thin films that are to be studied are cut into strips, a convenient way of applying stress is to use a four point bending fixture. According to the classical material beam theory, when a thin plate is loaded in a four point bending fixture a uniform stress field is formed over a large region of the specimen, see *Figure 3*. Further, in view of the simple geometric configuration of the fixture, the stresses in the material can easily be calculated [13]. For this reason, the wafers with the fabricated resistors were diced into chips with suitable dimension for measurement in a four point bending fixture configuration. To this end, an experimental set up was designed and constructed.

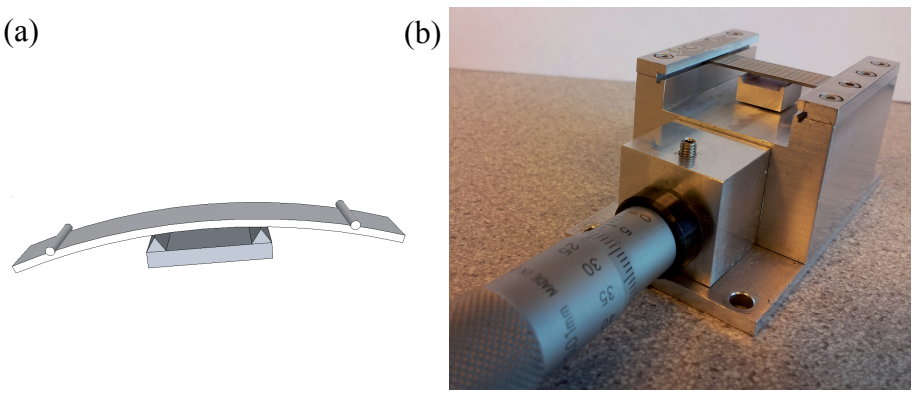

Figure 3. (a) Sketch of a 4-point bending fixture for applying mechanical stress (b) Picture of the 4-point bending fixture used in the experimental setup

2.3.2 Results

Initial measurements illuminated two notable difficulties which necessitated further studies.

Substrate bias

Since higher resistivity was preferred, a fairly low doping concentration was chosen. The conductance of the thin silicon film was therefore extremely sensitive to the applied backside voltage of the wafer, see *Figure 4*. The behavior is basically that of a field effect transistor where the resistor acts as the channel while the wafer substrate as the gate. When the backside voltage was decreased, the concentration of the charge carriers increased resulting in a corresponding decrease of resistivity. In the same way, if the voltage was high enough, the resistivity increased drastically and the resistor eventually became fully depleted and practically no current could consequently flow through the resistor. When 0V was applied, the thin films became nearly fully depleted and the resistance was in the order of gigaohms and therefore a negative voltage was applied during the measurements.

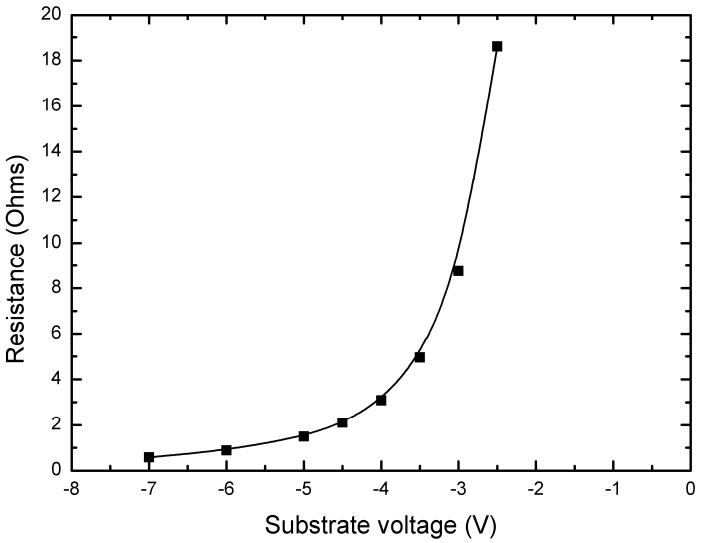

Figure 4. Resistance of silicon layer versus substrate voltage

Time drift

During prolonged measurements a drastic time drift in the measured signal was observed. As seen in *Figure 5*, the resistance drops dramatically during the first few minutes, but not even after more than 17 hours of measurement is steady state reached. It can also be seen from the figure that the resistance can be either increasing or decreasing during the time drift, even though the resistors originate from the same batch. Further investigations were made to explain the time drift behavior. C-V characterization measurements showed both depletion and inversion/accumulation behavior in the resistors which

was also confirmed by TCAD simulations. It is also clear from the simulations that for negative substrate bias, the silicon layer is accumulated with holes close to the buried oxide interface, while with positive substrate bias, the silicon layer is in inversion. It is, therefore, concluded that the resistance in the thin silicon layer is dependent on the degree of accumulation, which may be affected by an injected charge in the oxide. If the holes from the silicon layer are injected into the buried oxide, a drift towards higher resistance is expected. Additionally, a bias-temperature stress measurement was also employed to investigate the presence of mobile charges [12]. The mobile charge density in the buried oxide was calculated to be 1.2 x 10^{12} cm^{-2}, which may explain the drift towards a lower resistance. However, mobile charges were probably accidentally introduced during the fabrication process and should normally not be a problem.

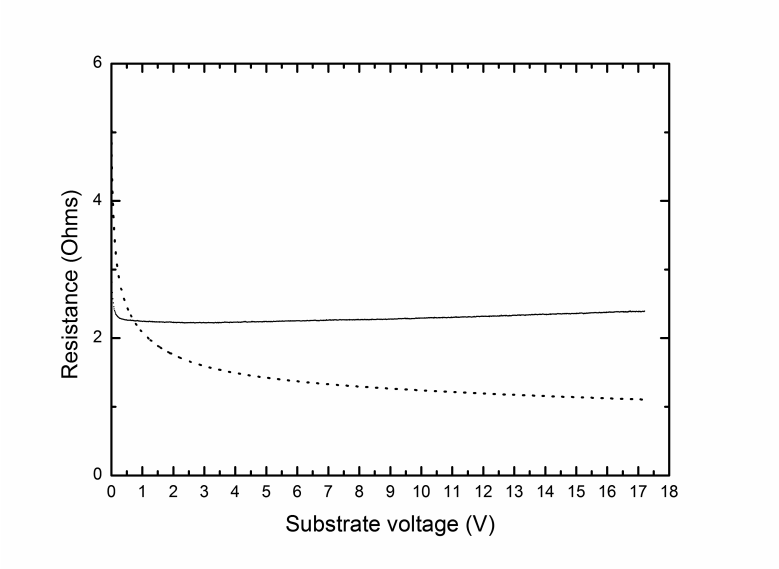

Figure 5. Long time drift of silicon resistors

The piezoresistive effect

Prior to measuring the piezoresistive effect, the thin film Si resistors were ”burned in” for several hours. A suitable substrate bias was chosen and a very small current, around 1nA, was driven through the resistor, which resulted in an almost zero resistance drift. A four point bending fixture was then used to measure the resistance as a function of the mechanical stress. The result is illustrated in *Figure 6* and the piezoresistive coefficient was very close to the bulk value of p-doped Silicon, i.e. the longitudinal piezoresistive coefficient $\pi_l = 71.8 \cdot 10^{-11}$ Pa^{-1}.

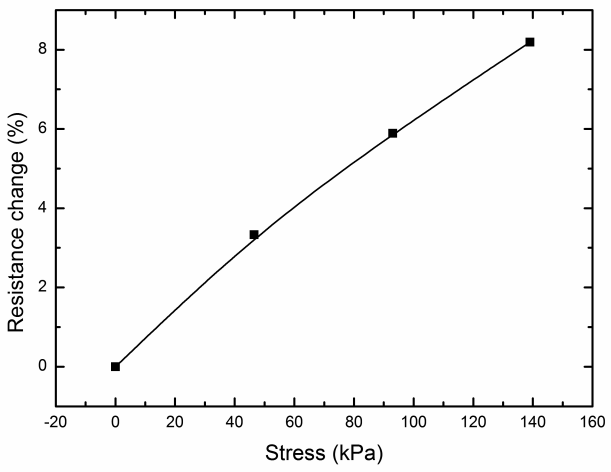

Figure 6. Resistivity change versus applied stress

2.3.3 The interface electron-trapping effect

Yang et al have manufactured thin silicon film resistors as well [14]. A thin silicon device layer on a SOI wafer was dry oxidized and subsequently the SiO_2 was removed with HF. This was repeated until desired thickness was achieved. A thin SiO_2 was finally grown as an insulating layer. The drawback using this approach is, as mention before, that the doping level in the resistors cannot be controlled, since the dopants diffuses into the oxide during the oxidation process.

Theoretical studies based on a two-dimensional quantum confinement effect model [15, 16] have predicted an increased piezoresistive effect in p-type nano thick silicon-layers. The conclusion was that the sensitivity in this case should exceed several times that of bulk silicon which prediction was later confirmed experimentally [9, 17]. However, Yang et al show that this is only true for relatively thick samples, thicker than 10 – 20 nm, depending on the fabrication process. It was shown that thinner silicon nano films can exhibit larger change in resistance compared to the predictions from the 2D confinement model. Both the transverse and the longitudinal GPR effect deviated significantly for thinner samples, especially the longitudinal which not only exhibited a higher value, but also a sign change as well.

Briefly, the suggested explanation is that at or near the Si/SiO_2 interface there are positive charges. These interfacial charges create an electrical field which causes the conduction and the valence band to bend near the interface. This band bending influences the carrier concentration in the silicon layer, which in this case means that the hole concentration decreases in the p-doped silicon near the SiO_2 interfaces. The interface charge is mainly com-

posed of oxide fixed charge and interface trapped charge. The traps near the interface may interact with silicon by capturing or emitting electrons [18]. It has been shown that an applied mechanical stress increases the electron trap density [19-24]. Therefore, under stress, the number of trapped electrons increases resulting in the neutralization of the positive interface charges. Hence, the band bending decreases and the hole charge carrier concentration increases near the interfaces, though never higher than the original doping. For thick samples, this interface effect can be neglected, while in a very thin sample, the film mainly consists of interfaces rather than bulk and this effect will be a major factor contributing to the resistance variation due to stress.

This explanation is in good agreement with the simulation and discussion made by Rowe [10].

3 Micro acoustic devices

Acoustic waves in solids exhibit two unrivalled properties, namely extremely low propagation losses and very low propagation velocities. The latter are five orders of magnitude smaller than the speed of light meaning that one can devise extremely compact electronic components in relation to the electromagnetic wavelength. Thus, by transforming electromagnetic waves into acoustic waves one can manipulate (process) signals in an efficient way before converting them back into an electromagnetic wave. The most common method to generate and detect acoustic waves involves the utilization of the converse and forward piezoelectric effect respectively. The field dealing with the science and technology of this phenomenon is called electro-acoustics. The applications of the electroacoustic technology range from frequency control, (filters, duplexers, resonators, delay lines, etc) through to sensors (physical, chemical and biochemical). Electroacoustic based sensors exploit the high sensitivity of the propagation characteristics of acoustic waves in solids with respect to various perturbations – stress, temperature etc. The remainder of this thesis studies membrane based resonators as pressure sensors.

3.1 Introduction to acoustic devices

3.1.1 Piezoelectricity

A piezoelectric material produces an electric charge when a mechanical stress is applied (direct piezoelectric effect). Conversely, a mechanical deformation is produced when an electric field is applied (converse effect). This phenomenon appears in crystals that have no center of symmetry. Most chemical bonds in a crystal exhibit some sort of a polarization, which means that one end is more negatively charged than the other forming in this way an electric dipole moment. When the crystal is unstrained, the charges in the crystal lattice are arranged in such a way that the net dipole moment is zero. However, when the crystal is strained, the ions of opposite signs are displaced relative to each other, producing a non-zero net dipole moment and thus an electrical polarization in the crystal. Conversely, the application of an external electric field interacts with the individual dipole moments resulting in a deformation of the crystal as a whole.

The piezoelectric effect may be strong for a given propagation direction while completely absent in another direction for a specific crystal and wave polarization. Polarization is induced by two types of stresses, namely compressive or shear, see *Figure 7*

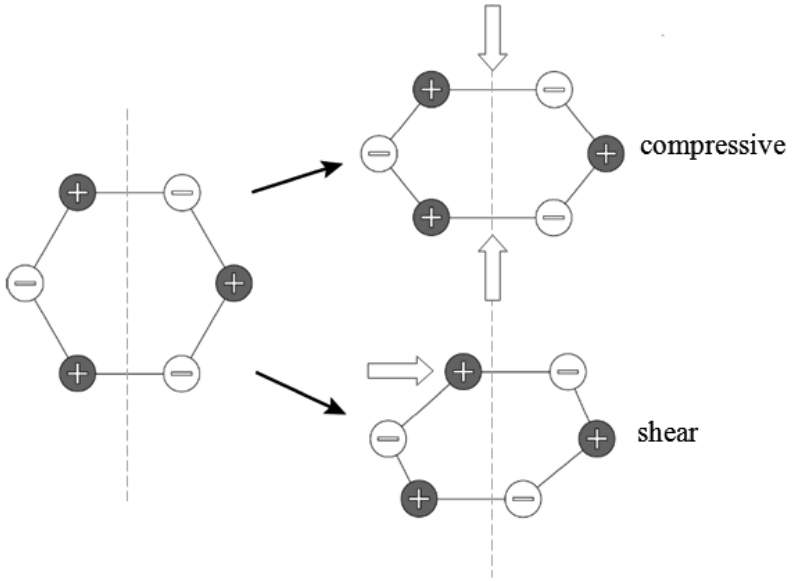

Figure 7. Schematic illustration of the piezoelectric effect.

The piezoelectric effect is the most common way to generate and to detect acoustic waves. In practical terms there are several figures of merit. Two of the most important is the electromechanical coupling factor k and the mechanical quality factor Q, also called the Q-factor. The electromechanical coupling factor is defined as the ratio:

$$k^2 = \textit{mechanical energy / electrical energy}$$

and represents a measure of the conversion efficiency between electrical and acoustic energy in piezoelectric materials. The quality factor Q in an acoustic device is a dimensionless parameter that is related to the overall losses in a device. It is defined as the ratio between the stored energy and the energy lost in one wave cycle. The higher the Q, the lower the energy loss relative to the stored energy, or in other words, the oscillations die out more slowly.

3.1.2 Acoustic wave theory

An acoustic wave in a solid is simply a periodic (in time and space) disturbance in the solid. This disturbance essentially represents displacements of

the particles from their steady state positions. In macroscopic terms this disturbance generates *strain (S)* and *stress (T)* in a material which quantities describe the corresponding mechanical deformations and associated internal forces, respectively. A plane wave generates displacements that vary harmonically in the direction of the wave propagation. Most generally, the relationship between S and T is rather complex, but for relatively small displacements higher order terms in this relationship can be neglected resulting in a linear dependence between S and T. In the one dimensional case this relationship, also known as the Hooke's law, is given by $T = cS$, where the constant c represents the stiffness constant. However, the complete representation of stresses and strains in solids requires an elastic coefficient tensor notation, but due to symmetries of the tensor, it can be reduced to a 6 by 6 matrix, which for most general solids consists of at maximum 21 independent constants.

In isotropic solids acoustic waves can have either longitudinal or transverse polarization, which generates compressional or shear deformation, see *Figure 8*. However, in anisotropic solids, quasi modes can exist with both longitudinal and transverse polarization components. Fluids, such as air or water, can only support longitudinal waves and therefore, for in-liquid applications a shear wave motion is required where the acoustic energy is confined to the resonator cavity, while avoiding acoustic leakage into the surrounding medium. However, due to frictional forces within the viscous media, the shear motion will always experience certain losses due to viscous damping.

Figure 8. Longitudinal mode and shear mode deformation through thickness excited actuation

3.1.3 Resonators

An electroacoustic transducer represents an electrode configuration that converts an electric signal into a mechanical wave and vice versa. The simplest example is where a piezoelectric material (a plate or a thin film) is sandwiched between two parallel metal electrodes, see *Figure 9*. When a voltage is applied to the electrodes, the electric field parallel to the thickness direction of the piezoelectric plate will deform the crystal according to the piezoelectric effect, generating in this way a bulk acoustic wave. It is a straightforward task to show that for any physical configuration of this transducer there exist specific frequencies at which the forward and the reflected waves interfere constructively, creating in this way an acoustic resonance. Accord-

ingly, this configuration is called a thickness excited bulk acoustic wave resonator (BAW).

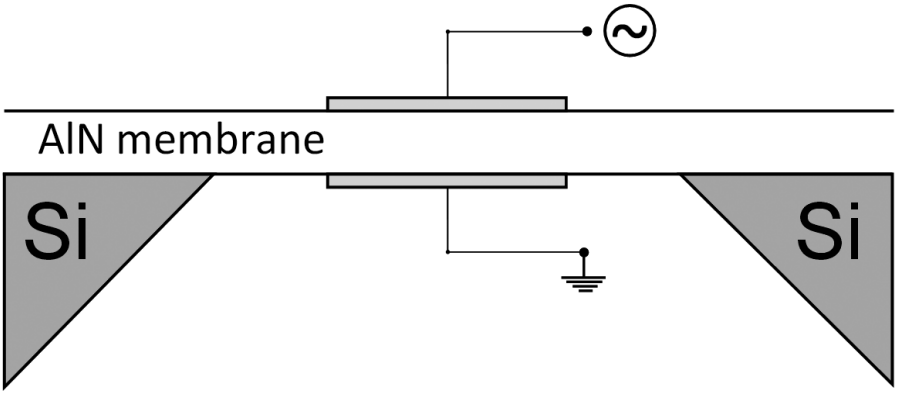

Figure 9. Sketch of an FBAR

More specifically, acoustic waves are generated between the electrodes and are subsequently reflected by the plate free surfaces. When the excited and the reflected waves interfere in a constructive manner, *mechanical resonance* occurs at a specific frequency also called *resonance frequency*. The resonance frequency depends on the resonator configuration, the material properties and the thickness. Consequently, the resonance frequency is directly affected by temperature and stresses, which makes the resonator suitable for sensor applications. Approximately the resonance occurs for frequencies given by the condition for wave synchronism $f = V / \lambda$, where V is the acoustic wave velocity and λ is the acoustic wavelength. This type of resonators operate at frequencies corresponding to standing waves defined at wavelengths $\lambda = 2d/n$, where d is the thickness of the resonator and n = 1,3,…2k+1 represents the harmonic of operation. Electrically only odd harmonics can be excited.

Further, it is also clear that the frequency of operation is inversely proportional to the thickness of the resonator. Traditionally, such resonators are made of single crystalline materials such as quartz, LNO, LTO, etc. Typical frequencies of operation are in the low MHz range. Thus, a thickness of the quartz crystal of 250 μm results in a resonance frequency of about 10 MHz. The lateral dimensions of such a resonator are of the order of 1 cm.

The explosive development of mobile telecommunications in the past two decades necessitated the use of microwave frequencies which lead to the development of the so called Thin Film Electroacoustic (TEA) technology. In essence, instead of thinning down single crystalline materials (which is an expensive operation) scientists developed synthesis processes for the deposition of thin piezoelectric films with thicknesses of the order of several microns. This also lead to a significant decrease of the lateral dimensions of the

resonators due to obvious impedance requirements. Thus, a typical thin film bulk acoustic resonator (FBAR) has lateral dimensions of the order of 200 μm. The miniature dimensions of these resonators require the use of a carrier substrate (typically Si or glass) which necessitates good acoustic isolation from this carrier substrate. This is achieved by either defining a cavity underneath the resonator or by using an acoustic Bragg reflector [25]. In the latter case the FBAR is often referred to as a Solidly Mounted Resonator (SMR).

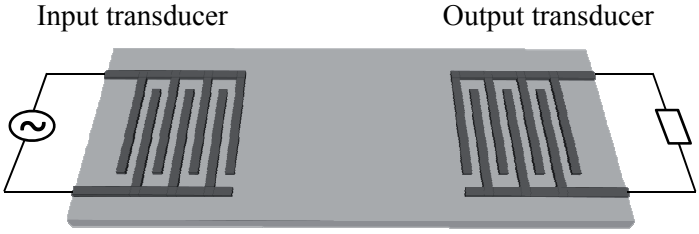

Figure 10. Surface acoustic wave resonator with interdigital transducers

Another common transducer type is the interdigital transducer (IDT) [26], which is a device that consists of two interlocking comb-shaped metallic structures, see *Figure 10*. One of the comb shaped electrode in the IDT is connected to ground, whereas an alternating voltage is applied to the other electrode. A periodic electric field in the near surface region is generated which produces a mechanical deformation propagating along the surface. IDTs are correspondingly used to convert the mechanical deformation back to an electrical signal. These transducers are typically used for the generation of surface acoustic waves (SAW).

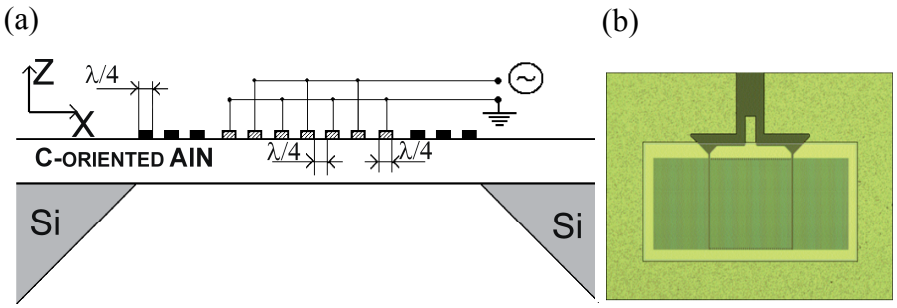

Figure 11. The FPAR sensor (a) sketch (b) picture

Recently, the IDT configuration has been employed for the excitation of *Lamb (*or *plate) waves* which propagate laterally in plates of thicknesses comparable or smaller than the acoustic wavelengths, see *Figure 11*. Resonators employing Lamb waves are called thin film plate acoustic resonators (FPAR). In such a configuration metal strip gratings can be used as reflectors

on both sides of the transducer. The reflected and the excited wave can interfere constructively to confine the acoustic energy and give rise to resonance.

3.1.4 Acoustic wave modes

Acoustic wave devices are often named after the acoustic wave (or mode) employed. Here follows a brief description of the wave modes employed in this thesis.

Bulk acoustic waves

There are basically two types of bulk waves, a longitudinal wave and a shear wave. In the former the particles oscillate in the direction of the wave propagation only, while in the latter the particle displacements are orthogonal to the wave propagation, see

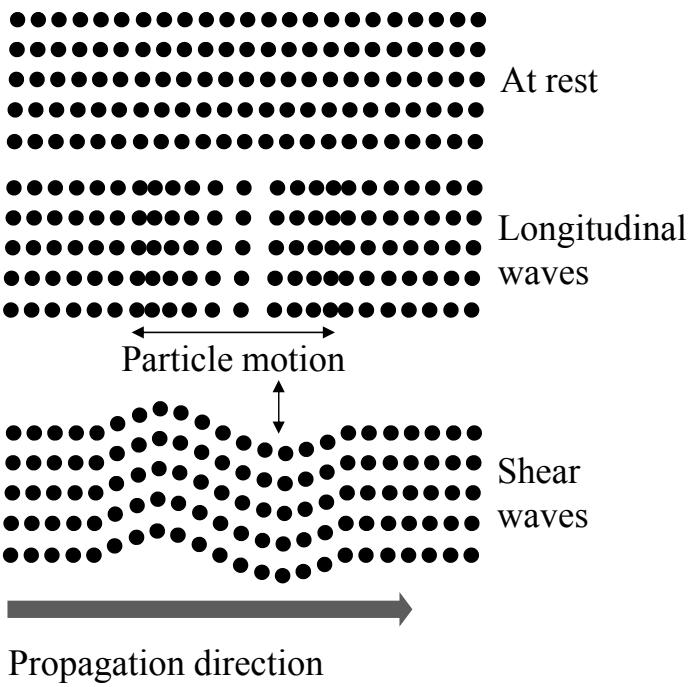

Figure 12. As described earlier, in certain materials, quasi modes with both a longitudinal and a shear component can propagate.

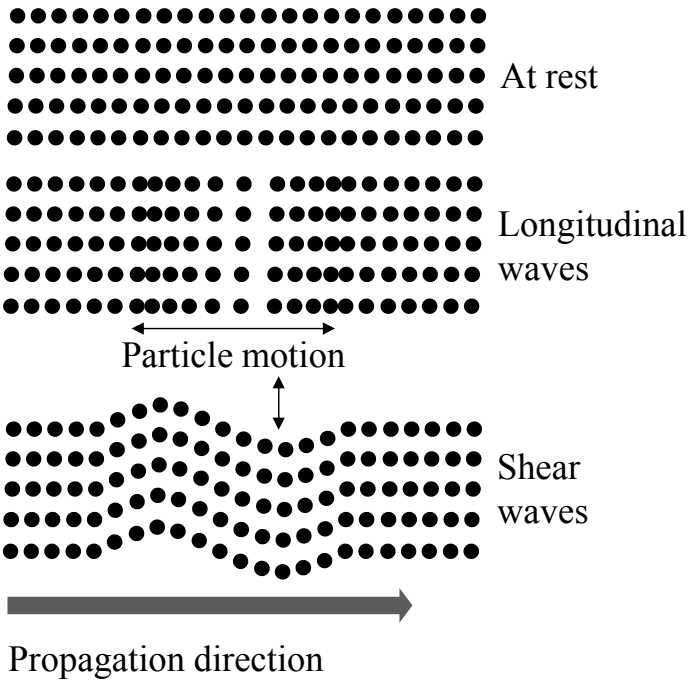

Figure 12. Schematic representation of longitudinal and shear waves

Surface acoustic waves

SAW devices employ surface acoustic waves, also called Rayleigh waves which represent a special type of wave confined to the surface of a solid. Thus, they propagate near the surface of the solid and include both longitudinal and transverse motions, see *Figure 13*. The amplitude of the wave decreases exponentially with depth. SAW waves are typically excited by the use of IDTs.

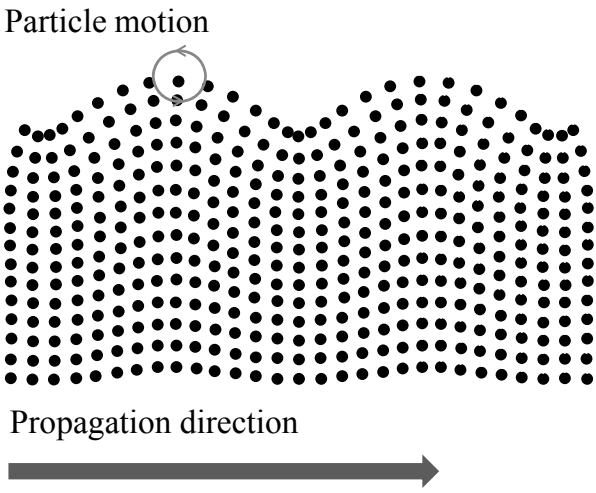

Figure 13. Schematic representation of surface acoustic waves

Plate waves

Plate waves are similar in nature to SAW waves. They typically are guided and propagate in thin plates, that is, plates with a thickness of the order or smaller than the acoustic wavelength. Plate waves are generally divided in two sub-groups, the shear plate acoustic modes (with transversal polarization) and the Lamb waves (with elliptical polarization including vertical shear and longitudinal displacements). Plate waves have generally two modes, symmetric and asymmetric, respectively, following the symmetry of the particle motion relative to the median plane of the plate. Obviously, in the first instance the particle motion is mirrored by the medial plane while in the second instance the particle motion on either side of the median plane is fully in phase, see *Figure 14*. The plate supports a number of these wave modes depending on the plate thickness to wave ratio. The different plate modes are denoted with letters. Thus for example, the n^{th} symmetric Lamb wave mode is denoted by S_n and the n^{th} asymmetric Lamb wave is denoted by A_n. This thesis deals specifically with the S_0, the A_1 and the S_1 Lamb modes.

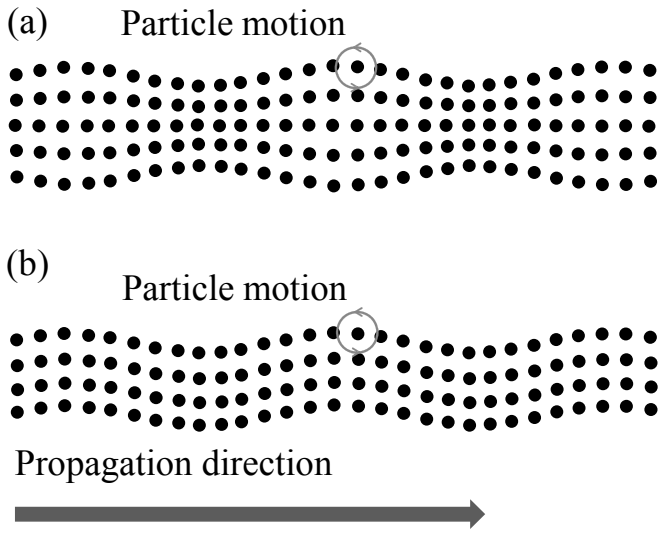

Figure 14. Schematic representation of Lamb waves, (a) symmetric and (b) asymmetric

3.2 Acoustic pressure sensors

3.2.1 A review

Acoustic wave devices have been in commercial use for more than 70 years. The largest application is by far acoustic wave filters in telecommunications and these are typically SAW devices. However, there are other applications for acoustic wave devices such as torque, pressure, vapor, temperature and mass sensors as well as chemical and biochemical sensors.

The MEMS pressure sensor market is still dominated by piezoresistive and capacitive pressure sensors. The first reported use of the SAW technology for sensor application was a pressure sensor [27]. The wave velocity in a SAW resonator is strongly dependent on the stresses in the piezoelectric substrate. Two IDTs, one transmitter and one receiver, were placed on a diaphragm. When pressure was applied, the diaphragm bends which induces stress in the latter and consequently introduces perturbations in the stiffness constants of the material. The net result is a change in the propagation velocity and hence in a variation in the delay time.

Another incarnation of this delay line concept represents an IDT that generates a wave pulse. The latter is reflected by suitable reflectors, placed at some distance along the propagation path, and is converted back to an electrical pulse by the same IDT. The reflectors can be configured in such a way that distance and acoustic wave velocity between them varies with applied pressure, e.g. on a membrane. Therefore, a partial phase or time shift in the

reflected pulses is then related to the applied pressure. Such sensors have been integrated into car tires for pressure monitoring [28]. These sensors are passive (no power is required) and can be wirelessly interrogated [29] which makes them suitable for measuring pressure in moving objects. These features offer advantages over capacitive and piezoresistive sensor technologies, which require power and are not wireless. Similarly, the same technology can be used as wireless torque sensors [30].

Until now scientific publications on pressure sensors employing BAW waves have been scarce. Since such sensors are mostly based on thick piezoelectric crystals (quartz), it is not economical to machine them down into thin membrane devices and thus they are not particular sensitive to pressure. However, the development of the thin film electroacoustic technology paved the way for the design and fabrication of miniature and highly sensitive BAW (and more specifically FBAR) sensors.

3.2.2 Pressure sensitivity

When analyzing the potential of electroacoustic based devices as pressure sensor, it is important to take a closer look at the major factors determining their pressure sensitivity. The first most important factor is represented by the *elastic constants* in the elasticity tensor $\boldsymbol{c}$ representing the proportionality constants in the three-dimensional formulation of Hook's law $T=cS$, where T is the stress tensor, S is the strain tensor. When a material is exposed to external pressure, the internal pressure changes correspondingly. The internal pressure is here defined as the mean negative internal stress ($P_{INT} = -(T_{XX} + T_{YY} + T_{ZZ})/3$). On the other hand, it has been shown by Lepkowski et al [31] that the elastic constants of materials and more specifically of aluminum nitride (AlN) depend on the internal pressure. As shown in paper IV och VI, the most important pressure sensitive property for both the FPAR and the FBAR modes is the variation in the elastic constants due to induced stresses, i.e. when the material is stressed as a result of applied pressure, the resonance peak is shifted for all modes studied, namely for the S0, A1 and S1 Lamb modes as well as for both the longitudinal and the shear thickness bulk acoustic waves.

Intuitively, if the material in which the waves propagate is strained, the resonance will be shifted due to changes in the geometrical dimensions of the resonating cavity as a result of the induced deformation. Thus, the propagation distance becomes either larger or smaller which naturally affects the waves, especially the highly dispersive modes (those for which the velocity depends strongly on variations in d/λ). Correspondingly, when a material is strained in one direction, it tends to be compressed in the other according to Poisson's ratio. In the membrane case, it means that when a pressure differential is applied, the membrane buckles, the material becomes laterally strained, which results in that the membrane becomes thinner. The latter

effect will affect the sensitivity of the modes that originates from the plate thickness resonances, such as the Lamb A1 and S1 modes.

The relative contributions to the pressure sensitivity in membrane resonators on the above three factors (the pressure dependence of the elastic constants, the lateral and vertical strain), have been studied and discussed in paper IV and VI.

3.2.3 Optimization of pressure sensitivity

It is clear from the previous paragraph that solidly mounted resonators or similar configurations would not be suitable for pressure sensors with high sensitivity. A pressure sensitive resonator requires that the material is allowed to sufficiently strain under pressure and thus stressed. For this reason, most commonly used configuration in pressure sensors is the membrane one, which has a large area-to-thickness ratio. The challenge to support very thin membranes has since long been solved with the highly developed MEMS technology where silicon substrates are used. The same technique used to manufacture capacitive or resistive pressure sensors can be used with the difference that the thin piezoelectric film itself defines the membrane.

One question that has to be addressed is: what aspect ratio is most optimal? A common trade-off in this context is that between size and sensitivity. The smaller the membrane, the lower the sensitivity, since the deformation of the membrane (and hence the stress induced) is proportional to the area-to-thickness ratio.

The next question to be addressed is: what material is the most suitable to use? As discussed earlier, the elastic constants of the material play an important role and their pressure dependence varies between different materials. Different crystal orientations in the piezoelectric materials determine the different wave modes that can be excited, which in turn have different pressure sensitivities. This has been studied and presented in paper VI.

Another very important question is: which modes are most sensitive to pressure? The sensitivity to strain of Lamb modes, for example, differs remarkably between the modes. Hence, the pressure sensitivities of four different acoustic modes have been studied and presented in papers IV and VI.

3.2.4 Additional considerations

Membrane based resonators are not only sensitive to pressure. Various other environmental factors may also influence the resonator operation. Of particular significance are various sources of noise (see section 3.3). Care must be taken to eliminate/minimize this noise which reduces the ultimate resolution of the sensor. Standard methods for noise minimization include differential measurements, temperature compensation, high quality factors etc.

Besides pressure sensitivity this thesis also includes additional studies of the mass sensitivity of the respective resonators as well as their ability to operate in liquids which is important in view of biosensor applications.

Mass sensitivity

The most common electroacoustic sensing application is the gravimetric principle for mass detection. A number of studies of the mass sensitivity of quartz crystal microbalance (QCM), SAW, FBAR devices have been presented in the literature [32-35]. The mass sensitive devices are mainly used as gas and bio-sensors where the device is coated with a specific gas sorption layer or a biorecognition layer. The analyte reacts (physically or chemically) with this layer, which leads to an increase of the overall resonator mass. The mass sensitive device can therefore be used as both gas and biochemical sensors to detect different gases, drugs, explosives etc.

In-liquid operation

In many sensor applications the device must operate in liquid environments. Whether an acoustic device can operate in a liquid depends on the level of acoustic wave radiation into the liquid in addition to the relative magnitude of the viscous losses. For example, the longitudinal waves BAW and SAW exhibit displacements perpendicular to the surface, which in turn generate compressional waves propagating into the liquid. This results in severe acoustic losses and thus severe Q degradation. However, waves with in-plane displacements, such as shear BAW do not propagate into the liquid. A special case, though, is the Lamb S0 mode which has predominant horizontal polarization, while the shear vertical displacement is by an order of magnitude smaller. This in combination with its much higher phase velocity than that of water acoustic emission into the liquid make the acoustic wave radiation into the liquid quite limited. Note that the acoustic Snells's law permits such a radiation, but its strength is small which in turn preserve the divece performance when operating in liquids.

3.3 Noise performance

One challenge when miniaturizing sensors is to maintain the efficacy from larger devices. In sensors, the noise sets the limit for the smallest acceptable size. It has been shown [36, 37] that the thermal noise energy is constant regardless of the size of the system. However, when the devices are scaled down, the signal power is usually lowered and eventually for small enough devices the signal level will fall below the thermal noise.

Noise in the frequency domain

The noise can be observed in the time or the frequency domain, where the latter often is of greater interest. In the frequency domain, the two most important frequency distributions are the white noise and the $1/f$ – noise. The most common white noise mechanism is the thermal noise and it is generally constant and independent of frequency. However, due to the finite bandwidth of any real system (for example wires working as filters or use of resonant sensors), the white noise will be shaped by it.

The $1/f$ – noise, also known as flicker noise, is inversely proportional to the frequency and is caused either by electrical mechanisms as random trapping and release of electrical carriers or by mechanical mechanisms for example in quartz crystals due to nonlinear forces and surface related effects [38, 39].

Signal-to-noise ratio

In a system the measured signal should be larger than the noise level, intuitively. To determine noise performance of a device, one must know the signal-to-noise ratio (SNR) which describes the signal quality. The SNR is defined as:

SNR = signal power / noise power

Using the SNR, the performance of two similar devices can be compared.

Determining the noise floor

Due to noise it is impossible to measure an exact instantaneous signal and therefore, a probability distribution for the measurement is considered. A probability that the signal will fall within a certain range can be calculated if the characteristics of the noise is known. For the most common noise sources, the probability follows the Gaussian distribution

$$f(v_n) = \frac{1}{\sigma_{rms}\sqrt{2\pi}} e^{-\frac{v^2_{measured}}{2\sigma^2_{rms}}} \tag{5}$$

where $v_{measured}$ is the measured signal and σ_{rms} is the standard deviation from the average signal. σ_{rms} where "rms" stands for "root mean square" is determined by taking the square root of the mean of the squares of the measured values, thus obtaining the statistical measure of the magnitude of the varying of the signal. The probability that the signal is between two certain values is obtained by integrating equation (5) between those values [40].

In the case with acoustic devices the measure of random fractional frequency fluctuations (or noise) is the Allan deviation and is measured in time domain [41]. The Allan deviation is defined as

$$\sigma_y(\tau) = \sqrt{\frac{1}{2}(\overline{y_{n+1}} - \overline{y_n})^2} \tag{6}$$

where τ is the observation time and $\overline{y_n}$ is the n_{th} fractional frequency average over the observation time. The minimum $\sigma_y(\tau)$ is inversely proportional to the Q of the device. Empirically the relationship between the Q value and the noise floor is [42].

$$\sigma_y(\tau) \geq \frac{1.0x10^{-7}}{Q} \tag{7}$$

Noise in piezoresistive devices

A great disadvantage with piezoresistive devices is the added noise from the resistors. The thermal noise in resistors is linearly dependent on the resistance itself and the only way to increase the SNR where the noise is dominated by thermal noise, is to increase the measurement power, which could be disadvantageous especially in battery powered sensors. Additionally the $1/f$ – noise could be high at dc or low frequency measurements. The $1/f$ – noise is also inversely proportional to the resistor volume and physically large resistors may be needed for low noise design. One way to decrease the $1/f$ – noise is to increase the doping density, which at the same time reduces the piezoresistivity. Another noise source in resistors is the so called *shot noise* which occurs due to random fluctuations of the electric current across a potential barrier. Ideal resistors do not exhibit this noise, however it may occur due to bad contacts.

Noise in RF acoustic devices

As described in reference [43] there are several noise sources in an acoustic device, such as noise due to motional resistance (Johnson noise), thermal response, stress reliefs at interfaces, acoustic noise and vibrations, mass and viscous loading, etc. Moreover, it has been shown that the minimum noise in a resonator is inversely proportional to its Q value, which is also known to decrease with frequency as Q~1/f i.e. the higher the frequency, the higher the noise floor [42].

3.4 Summary of papers regarding acoustic devices

In this part of the thesis, the pressure sensitivity of FPARs and FBARs have been theoretically and experimentally studied. The focus of the study has been the main factors determining both the sensitivity and the resolution of an acoustic membrane cavity, that is membrane aspect ratio, type of material, acoustic modes, etc.

Briefly, when pressure is applied to a membrane, it is being strained, which causes stress which in turn causes the elastic constants to change. This elastic constant change and the deformation of the membrane itself causes a shift in the resonance frequency. This shift, due to applied pressure can be measured using the methods described below. The contribution to the resonance frequency shift from the lateral strain, the vertical strain and the change in the elastic constants as well as the energy distributions of the wave in the plate can be simulated using the numerical methods listed below.

3.4.1 Methods

Thin film synthesis

The piezoelectric material used in the resonators is wurtzite aluminum nitride and has been deposited using a von Ardenne reactive magnetron sputter deposition system. Both c-axis and c-tilted thin films were deposited using the same system. The c-tilted film was grown in a two step process varying the process pressures described by Bjurström et al [44].

Electrical characterization

The electrical characterization of the resonator devices was made with a HP8364B network analyzer equipped with G-S-G pico-probes and controlled by MATLAB.

To be able to apply pressure to the resonators a special fixture was made, see *Figure 15*. The fixture was designed to accommodate chips with lateral dimensions of 6 mm x 6 mm. Each such chip contained a single resonator to be tested. The chips were mounted into the fixture by firmly pressing them against an o-ring lubricated with vacuum grease. The fixture was then connected to a pressure system including a hydraulic accumulator together with pressure regulators and flow control valves. A digital pressure indicator GE Druck DPI 705 was used to monitor the pressure.

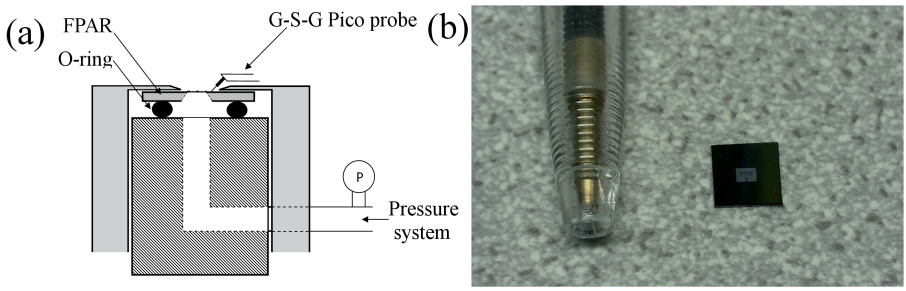

Figure 15. (a) Cross section of the fixture for pressure measurements. (b) 6 mm x 6 mm FPAR chip.

Simulations

Finite element method (FEM) analysis using COMSOL Multi-physics was used to simulate the resonator behavior under external pressure. The membrane deformation, the internal pressure as well as how it contributed to the pressure sensitivity for different wave modes was simulated using both 2D- and 3D-models.

3.4.2 Sensitivity features of FPARs

[Paper III]

An FPAR operating at the S0 Lamb mode is sensitive to various external loadings and here a compilation of various sensitivity characteristics are presented.

The mass sensitivity towards SiO_2 mass loading layer of the S0 mode has been calculated using Adler's approach. The same mode has further been experimentally measured by coating the FPAR with SiO_2 thin films of various thicknesses. The frequency shifts have been used to determine the relative sensitivity, see *Figure 16*. It should be noted that both the Q value and the device response have remained unaffected by the layer deposition, which suggests that FPAR coated with sensing layers could be used as high resolution gas sensors.

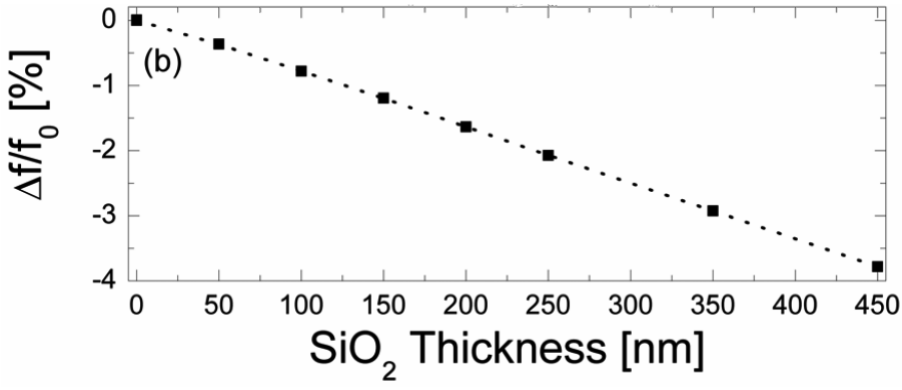

Figure 16. Fractional frequency shift vs SiO_2 layer thickness in an FPAR

The pressure sensitivity and the in-liquid operation measurements are further presented.

The conclusion is that the S0 Lamb wave in thin film membranes offers a unique combination of a weak dispersion, low noise as well as high sensitivity to both mass and pressure and its ability to operate in liquid environments could be employed in integrated biosensor applications.

3.4.3 Pressure sensitivity study of FPAR

[Paper IV]

In this paper the pressure sensitivity of AlN FPARs has been studied. The 12µm wavelength FPAR exhibits the S0, A1 and S1 Lamb wave modes at resonance frequencies of around 0.9, 1.6 and 2.26 GHz, respectively. The resonator is a micromachined one-port FPAR with an IDT transducer having reflectors symmetrically placed on either side. The thickness of the AlN membranes was 2 µm.

The membrane deformation was studied by FEM analysis assuming large strains. The total displacement of the FPAR membrane subjected to an ambient pressure differential of 50 kPa is shown in *Figure 17*. For all calculations within this study the ambient pressure difference was fixed to 50 kPa. The FEM model was further used to determine both the pressure distribution inside the membrane itself as well as the lateral strain and the vertical strain throughout the membrane.

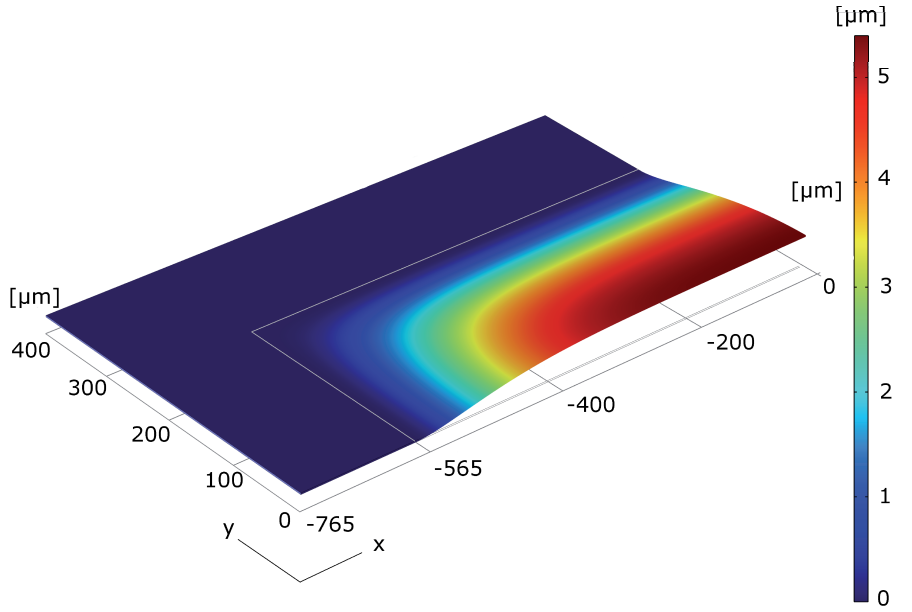

Figure 17. FEM simulation of the total displacement of an FPAR membrane under 50 kPa ambient pressure difference

Prior to determining the contributions of the various strains to the pressure sensitivity, the electro-mechanical energy density distribution in the membrane (in both X- and Y-directions) for all wave modes had to be determined. This was made through 2D and 3D wave FEM analysis in a comple-

mentary manner. The results indicate that all modes tend to store their energy in the vicinity of the membrane center.

To clarify the contributions of the different quantities to the pressure sensitivity of each mode, we have performed the eigen-frequency analysis of a single period FPAR cell, applying periodic boundary conditions. In this analysis the lateral strain, the vertical strain and the change in the elastic constants was introduced. The expected contributions to the pressure sensitivities of each FPAR mode as determined by the FEM analysis are shown in *table 1*. Note that the highest impact on the pressure sensitivity is provided by the stress-induced changes in elasticity and that the contributions related to the vertical strain are of opposite signs to the rest since the deformation is compressive in that direction. Further, the low dispersive S0 mode demonstrates the highest sensitivity to lateral strain, while the S1 mode being close to the zero group velocity dispersion demonstrates a marginal sensitivity. The opposite sign of the vertical strain determines the relatively smaller pressure sensitivities of the A1 and S2 modes as compared to the S0 mode. From the analysis, we conclude that the most pressure sensitive mode in the system is expected to be the S0 Lamb wave.

Table 1. *Contributions to the Pressure sensitivities of each FPAR mode at a 50 kPa ambient pressure difference*

Δf/f [ppm]	Lateral strain	Vertical strain	Internal pressue	**Total**
$\mathbf{S_0}$	-46.6	1.7	-178.7	-223.6
$\mathbf{A_1}$	-11.9	65.4	-133.9	-80.4
$\mathbf{S_1}$	-2.44	84.9	-188.9	-106.4

The measured sensitivities of the different FPAR modes are shown in *Figure 18*, and the results are in good agreement with the predicted values. Further measurements with pressure differences of up to 160 kPa exhibit linear pressure dependence without any hysteresis.

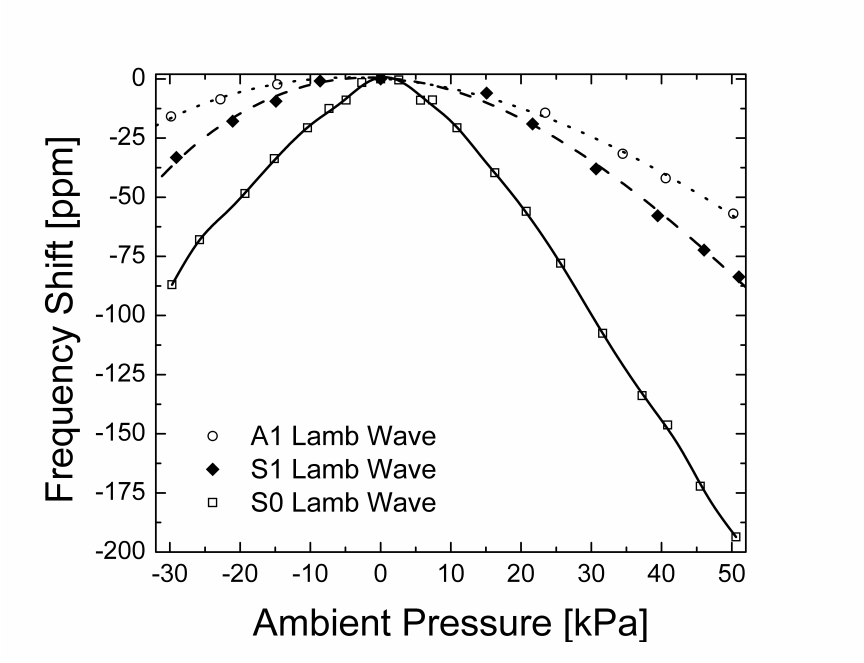

Figure 18. Measured pressure sensitivity of the different FPAR modes

3.4.4 Mass sensitivity of FPARs and ability to operate in liquid

[Paper V]

In this paper further studies on the FPARs have been performed. The pressure sensitivity together with the temperature sensitivity is presented for the S0, A1 and S1 modes in comparative manner. A differential pressure measurement between the S0 and A1 modes is proposed which could exclude the temperature drift due to their similar temperature sensitivity.

Further, the mass sensitivity of the resonators has been studied by calculating the frequency variation as a function of mass loading with ultrathin SiO_2 layers. The relative sensitivity of the S0 mode was calculated to be substantially higher than that of SAW devices at the same wavelength of λ=12 μm. The fractional sensitivities of the A1 and S1 mode are expected to be higher, see *Figure 19*, but their sensitivity towards technological tolerances may limit their use in practical applications.

The FPAR performance has been experimentally measured in contact with viscous liquids (water and a 50% glycerol solution, respectively). Both the highly dispersive A1 and S1 modes attenuate almost completely, while the S0 mode showed a sufficient performance. Specifically, the S0 mode demonstrated Q values of 1700 in air, 150 in water and 70 in the glycerol solution, respectively. Thus, FPAR devices operated in the S0 mode seem to be promising candidates for biosensor applications as well as for pressure sensors for in-liquid environment.

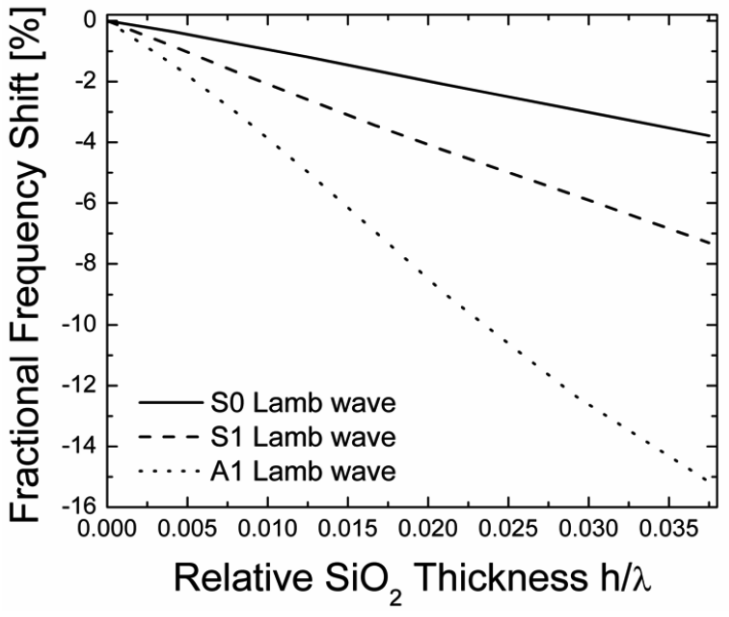

Figure 19. Mass sensitivity of the different FPAR modes

3.4.5 Pressure sensitivity of FBARs with c- and tilted c-axis texture

[Paper VI]

Another resonator configuration is the FBAR. In this paper FBARs with both c-textured and c-tilted AlN thin films, respectively have been studied. In other words, we study the longitudinal and the shear thickness excited modes respectively. Typical frequency responses of both the longitudinal and the shear FBARs are shown in *Figure 20*. The shear mode is in fact quasi-shear and has two components, namely one shear and one longitudinal.

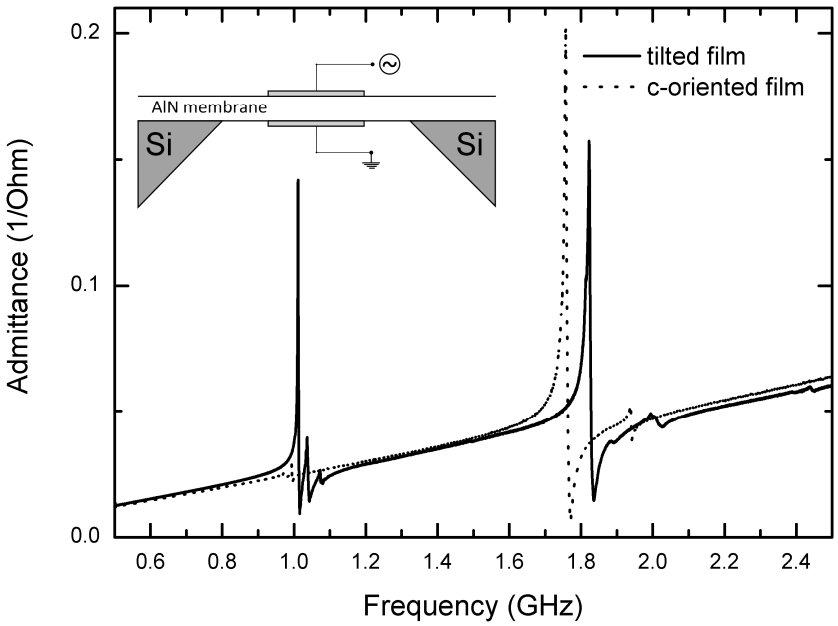

Figure 20. The frequency responses of two FBARs with a c-oriented and a c-tilted film respectively. The insert shows a cross section of the measured FBAR topology.

Finite element analysis has been performed to deduce the internal pressure at the membrane center under external ambient pressure differential. This has been done to eliminate both the membrane scaling and the effect of crystal anisotropy. In *Figure 21* the relative pressure sensitivity of the fundamental resonances in the different films are shown as a function of the internal pressure and thus the results show the pressure sensitivity at equal stress levels independent of texture and thickness variations in the membrane.

Further, shear FBARs in tilted c-axis AlN, operating at the fundamental shear resonance, demonstrate the highest sensitivity as compared to all other acoustic modes including the FPARs above. The results are coherent with the results from direct measurements of the relative frequency variation as a function of the applied ambient pressure differential, which indicates that the

improvement in pressure sensitivity is to a large extent determined by the improved pressure dependence of the shear elastic constants in tilted c-axis AlN films.

In addition, it has been shown that the shear mode has a high performance in contact with water (in terms of Q value), which makes the shear FBARs attractive for operating both in air and in liquid environments.

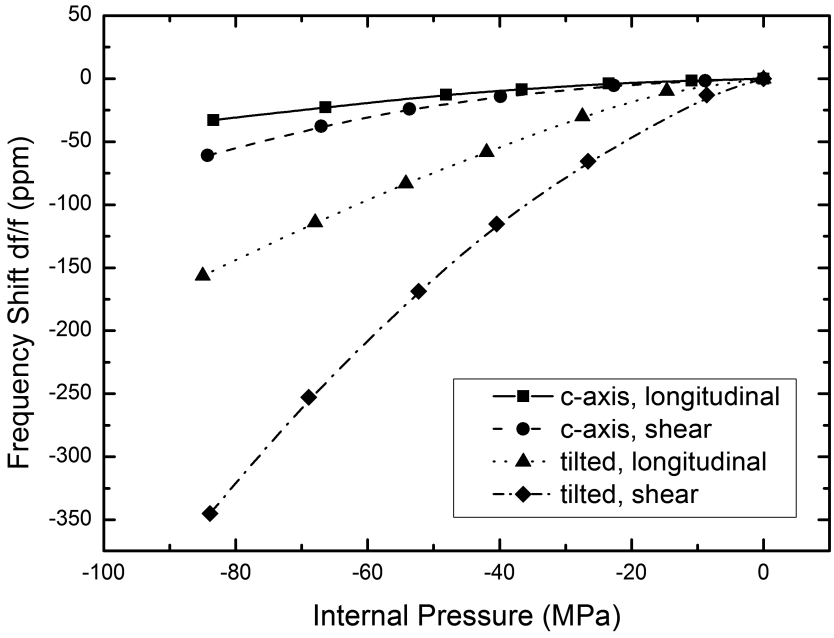

Figure 21. FBAR pressure sensitivity

3.5 Concluding discussion

This thesis presents work on different MEMS based pressure sensor designs where the main goal has been to either determine the pressure sensitivity or to increase it. Ways to increase the sensitivity in the well known piezoresistive pressure sensor have been examined. Furthermore, different pressure sensitive resonator designs operating with different acoustic wave modes have been thoroughly studied.

The piezoresistive coefficient

The piezoresistivity coefficient π in a material is defined by equation (4) where ρ is the resistivity defined by equation (3) where n and p is the carrier concentration and $\mu_{n,p}$ is the mobility. As mentioned earlier, piezoresistivity has traditionally been referred to as a mobility change in a piezoresistive material due to stress, for example in silicon. The change in carrier concentration in ordinary piezoresistors under stress has been negligible since it only occurs at the surface or at an interface. However, in the case where the resistors are scaled down to nano-size, as nano thin films or nanowires, the surface effects begin to take over the bulk effects and the carrier concentration becomes important.

Sensitivity and resolution

An important topic in sensor research has always been to increase the sensitivity of sensors. However, in real application the important figure of merit is actually the resolution. A sensor with *increased sensitivity* has often been referred to as an *improved sensor*, which is not necessary the case. As stated in equation (1), the resolution depends on the smallest detectable signal δ. Very often when sensitivity is increased, trade-offs have to be made resulting in higher noise or lowered reliability [42]. For example, as mentioned in section 3.3, miniaturizing a sensor could increase the sensitivity, while making it more sensitive to thermal noise, or when the sensitivity of an acoustic sensor is increased by increasing the frequency (decreasing its dimensions), at the same time, the noise, hysteresis and the aging, respectively, may be worsened [42]. The sensitivity may be increased, but nothing is actually gained in terms of usability unless the new design leads to increased resolution. Clearly decreased dimensions lead in both cases considered to higher noise. Resolution is gained only when the increase in sensitivity is higher than the corresponding increase in noise.

The case with acoustic sensors, however, is somewhat special since the definition of sensitivity is somewhat different. One of 15 definitions used in reference [45] reads: (regarding measuring devices) *"The ratio of magnitude of its response to the magnitude of the quantity measured"* which is not a suitable definition dealing with acoustic sensors. The unit would then be Hz per unit of measurand, which has often been used to report sensitivity. Com-

paring sensitivity between two pressure sensors operating at different frequencies would be meaningless. Throughout the work presented in this thesis regarding acoustic sensors, the relative magnitude of the response per unit of measurand has been used to be able to compare the different sensors operating at different modes at different frequencies.

High sensitivity in piezoresistive sensors

It has been reported a giant increase in the piezoresistivity in nanowires and nanofilms compared to ordinary bulk single crystalline and polycrystalline silicon. One should keep in mind that it does not automatically mean sensors with higher resolution. In this thesis it has been reported that working with nano-size structures may include various instabilities, such as time drift etc. As described in section 3.3, various noise sources could be enhanced when systems are made smaller. Since rather new techniques are used to fabricate the nano structures and very high precision is required, it is still hard to make industry compatible devices. To be able to manufacture sensors with higher resolution, it is essential to find ways to make robust sensors with high reproducibility and maintaining low noise while increasing the sensitivity.

Resolution in acoustic sensors

It has been stated in the sensor literature that high frequency sensors often exhibit higher sensitivity than low frequency devices. On the other hand it has been shown that higher-frequency resonators exhibit higher noise due to material and manufacturing technology [43, 46]. In reference [43] several different noise sources in acoustic devices are discussed. It has been shown that the minimum noise in a resonator is inversely proportional to its Q value i.e. the higher the frequency, the higher the noise floor [42]. Therefore, when the frequency is increased to enhance the sensitivity, more sources for noise are introduces and the final product may not exhibit higher resolution.

As an example the sensitivity and the resolution from the Lamb device and the FBAR from paper IV and paper VI, respectively, are presented in *table 2*. Preliminary resolution measurements were made using the Allan deviation approached mentioned in section 3.3. (it should be noted that since the dimensions differ between the two dimensions, the sensitivity and resolution values cannot be directly compared).

Table 2. *Pressure sensitivity and resolution in Lamb and FBAR devices*

Mode	Sensitivity [ppm/hPa]	Resolution [Pa]
S_0 - Lamb	0.382	34
Shear – tilted	0.441	124

It is clearly seen in this example that the sensitivity and the resolution do not automatically correlate. Here the sensitivity of the FBAR is higher than that

of the FPAR, though the FPAR pressure sensor has a much smaller resolution. This tells us that the noise in the Lamb devices is much lower compared to FBAR devices and therefore possesses great potential for making high resolution pressure sensors.

Sammanfattning på svenska

Med mikrosystemteknik (MEMS) kan man idag tillverka billiga, miniatyriserade sensorer som förbrukar mindre energi och ibland till och med visar högre prestanda än konventionella sensorer. Inom trycksensorer domineras marknaden av just MEMS-sensorer där dess största användningsområden är i bilindustrin och i elektronik för medicinskt bruk. Det sägs även att trycksensorer kommer att integreras i smartphones och surfplattor som höjdmätare och förutspås därför att inom en snar framtid vara den vanligast förekommande MEMS-enheten.

Den här avhandlingen inkluderar studier från två olika spår inom MEMS-teknik. Den första handlar om att förbättra känsligheten i piezoresistiva trycksensorer, medan den andra innefattar känslighetsstudier av olika akustiska sensorer.

Den vanligaste trycksensortekniken som används idag bygger på den piezoresistiva effekten. Av produktionsskäl används oftast polykristallint kisel vid tillverkning av piezoresistiva resistorer. Den piezoresistiva effekten i polykisel är dock förhållandevis låg. Det pågår därför forskning för att hitta sätt att öka denna effekt. Inspirerad av de senare upptäckterna av den enorma piezoresistiva effekten hos kisel-nanotrådar, antogs att liknande effekter skulle uppvisas av nano-tunna kiselfilmer. En metod att tunna ner kiselfilmmer togs därför fram och genom vanlig mikrostrukturteknik tillverkades diverse teststrukturer för mätning av piezoresistivitet. Det visade sig dock tidigt att mätandet av tunna strukturer innebar vissa svårigheter. Konduktiviteten i de tunna filmerna visade sig vara väldigt känsliga för vilken potential baksidan av substratet hade och betedde sig därmed som fälteffekttransistorer. En kontrollerad substratspänning fick därför appliceras.

Nästa svårighet som visade sig var tidsdrift under mätningarna. Under de första minuterna av mätningarna minskade resistansen drastiskt för att sedan plana ut, men efter till och med flera timmars mätande nåddes aldrig stationärt tillstånd.

Svårigheterna till trots uppmättes ingen piezoresistiv effekt som överskrider den för enkristallint kisel. Slutsatsen blev den att för att uppmäta en förhöjd piezoresistiv effekt måste tunnare filmer användas, vilket bekräftas av senare forskning som visar att kring 20 nm ligger den övre gränsen för filmtjockleken.

Den andra studien som har gjorts i avhandlingen handlar om tryckkänsligheten hos akustiska resonatorer. Två olika strukturer tillverkades och tes-

tades där båda består av en 2µm tjock aluminiumnitridfilm som bildar ett tunnt membran, medan det som skiljer dem åt är konfigurationen av elektroderna. I det lite mer simpla resonatorn ligger det en elektrod på vardera sidan om filmen för att excitera vågor i densamma och sätta resonatorn i resonans. Dessa strukturer kallas FBAR (thin film bulk acoustic wave resonator). Vid vanlig c-orienterad aluminiumnitrid kan endast långitudinella vågor exciteras. Om däremot kristallens c-axel är vinklad gentemot planets normal, kan även shear-vågor exciteras. Första ordningens långitudinella resonans och shear-resonans både för c-orienterad och vinklad aluminiumnitrid testades för tryckkänslighet genom att applicera ett kontrollerat lufttryck på membranet och sedan mäta frekvensskiftet. Shear-moden för vinklad aluminiumnitrid uppvisade högst tryckkänslighet och på grund av vågrörelsens natur, överförs inte vågens energi in i dess omgivande medium, vilket gör dessa komponenter lämpliga att användas i vätska.

Den andra resonatorn har en lite mer avancerad elektrodkonfiguration med en aktuator av tunna ”fingrar” som exciterar vågor och liknande reflektorer som begränsar vågenergin till ett inneslutet område. Dessa kallas för Lamb-resonatorer. I dessa kan flera olika vågmoder exciteras. Lamb-vågor brukar benämnas som antingen *symmetriska* (S) eller *asymmetriska* (A) där första ordningens skrivs S0 respektive A0, andra ordningens S1, A1 etc. De moder som undersöktes var S0, A1 respektive S1. Vid mätningar visade S0-moden upp störst tryckkänslighet. Även denna resonator testades för användning i vätska och S0-moden var den som visade tillräckligt bra resultat för att vara lämplig att användas i vätskemiljöer. Dessutom visar S0-moden upp god prestanda vid tester för masskänslighet, vilken även gör den lämplig i biosensor- och gassensorapplikationer.

En diskussion som också förs i avhandlingen är vikten av att mäta, inte bara känslighet, utan även upplösning. Inte helt sällan introduceras brus i samband med att känslighet ökar. Till exempel, när strukturer skalas ner för att öka känsligheten, måste man ofta minska effekten i kretsarna vilket gör systemet mer känsligt för termiskt brus. Och för akustiska komponenter ökas ofta känsligheten genom att resonansfrekvensen höjs, vilket samtidigt kan leda till sämre upplösning på grund av att brus i materialen i sig ökar. Slutsatsen är den att bara för att *känsligheten* hos en sensor ökas, behöver inte dess *upplösning* eller *prestanda* öka.

Utmaningen är att behålla lågt brus, men samtidigt öka känsligheten. Lamb-resonatorer har uppvisat lågt brus och här har det visats att de dessutom har god känslighet för tryck vilket gör dem till goda kandidater för tryck-sensorer med hög upplösning. Tack vare deras design lämpar de sig bra som passiva trådlösa sensorer, vilket ökar användningsområdet ytterligare.

Aknowledgement

I am happy that a doctoral thesis is not a one man show, but a team work with many contributing members and that those contributions does not necessarily have to be directly work related. A nice conversation over a cup of tea, a debate regarding existential issues at Facebook or company at the massage chairs in the basement could be undoubtedly important. I would therefore like show my greatest gratitude to…

…my supervisors *Ilia Katardjiev, Ventsislav Yantchev* and *Jörgen Olsson.* Ilia for supervision and for realization of my Ph.D. work, Ventsi for oracle like knowledge and for showing me how to surf through life with minimum effort and Jörgen for teaching me how to run hills until vomiting.

…my co-workers in the thin film group, *Lina* and *Lilja.*

…the people at Radi / SJM for realizing this work and for support, *Lars Tenerz, Leif Smith, Stefan Tiensuu* and many more.

…*Marianne Asplund* for dealing with the incomprehensible bureaucracy of Uppsala University, always with a smile.

…*Erik Särhammar* for always sharing his innermost questions.

…all the other colleagues at SSE.

…to my wonderful wife *Eva Anderås* for support and for entering a lifelong marriage together with me.

…my parents, brother and sisters for love and support.

…my Lord and God (yes I believe he exists) for leading me right and for convincing me that there is more to this world than what science can comprehend.

Bibliography

1. Dixon, R. Pressure Sensor to Become Top MEMS Device by 2014. 2011.
2. Smith, W.P.E.a.J.H., Micromachined pressure sensors: review and recent developments. 1997. p. 530.
3. Mosser, V., et al., *Piezoresistive pressure sensors based on polycrystalline silicon.* Sensors and Actuators A: Physical, 1991. **28**(2): p. 113-132.
4. Natarajan, K.S.a.N.D.a.K.N.B.a.K., Sensitivity enhancement of polysilicon piezo-resistive pressure sensors with phosphorous diffused resistors. 2006. p. 216.
5. Geyling, F.T., *Semiconductor Strain Transducers.* The Bell System Technical journal, 1960.
6. Petersen, K., et al., *Ultra-stable, high-temperature pressure sensors using silicon fusion bonding.* Sensors and Actuators A: Physical, 1990. **21**(1-3): p. 96-101.
7. Chung, G.S., et al., *Novel pressure sensors with multilayer SOI structures.* Electronics Letters, 1990. **26**(12): p. 775-777.
8. He, R. and P. Yang, *Giant piezoresistance effect in silicon nanowires.* Nat Nano, 2006. **1**(1): p. 42-46.
9. Reck, K., et al. Piezoresistive effect in top-down fabricated silicon nanowires. in Micro Electro Mechanical Systems, 2008. MEMS 2008. IEEE 21st International Conference on. 2008.
10. Rowe, A.C.H., *Silicon nanowires feel the pinch.* Nat Nano, 2008. **3**(6): p. 311-312.
11. Elwenspoek, M. and R.J. Wiegerink, *Mechanical Microsensors*. 2001: Springer.
12. Dieter, K.S., Semiconductor Material and Device Characterization. 1998: Wiley.
13. Gee, S.A., V.R. Akylas, and W.F. van den Bogert. The Design And Calibration Of A Semiconductor Strain Gauge Array. in Microelectronic Test Structures, 1988. ICMTS. Proceedings of the 1988 IEEE International Conference on. 1988.
14. Yongliang Yang and Xinxin, L., Giant piezoresistance of p-type nano-thick silicon induced by interface electron trapping instead of 2D quantum confinement. p. 015501.
15. Ivanov, T., et al., Quantum size aspects of the piezoresistive effect in ultra thin piezoresistors. Ultramicroscopy, 2003. **97**(1-4): p. 377-384.
16. Zhang Jiahong, H.Q.a., Yu Hong,and Lei Shuangying, *A Theoretical Study of the Piezoresistivity of a p-Type Silicon Nanoplate.* Journal of Semiconductors, 2008. **05**.

17. Toriyama, T. and S. Sugiyama, *Single crystal silicon piezoresistive nano-wire bridge.* Sensors and Actuators A: Physical, 2003. **108**(1-3): p. 244-249.
18. Nicollian, E.H. and J.R. Brews, *MOS (metal oxide semiconductor) physics and technology*. 1982: Wiley.
19. Teverovsky, A., *Effect of Mechanical Stresses on Characteristics of Chip Tantalum Capacitors.* Device and Materials Reliability, IEEE Transactions on, 2007. **7**(3): p. 399-406.
20. Shimoyama, N.M., Katsuyuki; Shimaya, Masakazu; Kyuragi, Hakaru, *Stress-induced device degradation due to die-attachment process after area bump formation.* Japanese Journal of Applied Physics, 1999. **38**(4b): p. 2262.
21. Hamada, A. and E. Takeda. *AC hot-carrier effect under mechanical stress [MOSFET]*. in *VLSI Technology, 1992. Digest of Technical Papers. 1992 Symposium on*. 1992.
22. Tuttle, B. and C.G. Van de Walle, *Structure, energetics, and vibrational properties of Si-H bond dissociation in silicon.* Physical Review B, 1999. **59**(20): p. 12884-12889.
23. Hamada, A. and E. Takeda, *Hot-electron trapping activation energy in PMOSFET's under mechanical stress.* Electron Device Letters, IEEE, 1994. **15**(1): p. 31-32.
24. Yount, J.T., P.M. Lenahan, and P.W. Wyatt, *The effects of thermal nitridation and reoxidation on the interfacial stress and structure of silicon dioxide gate dielectrics.* Journal of Applied Physics, 1995. **77**(2): p. 699-705.
25. Newell, W.E., *Face-mounted piezoelectric resonators.* Proceedings of the IEEE, 1965. **53**(6): p. 575-581.
26. Ballantine, D.S., *Acoustic Wave Sensors: Theory, Design, and Physico-Chemical Applications*. 1997: Academic Press.
27. Cullen, D.E. and T.M. Reeder. *Measurement of SAW Velocity Versus Strain for YX and ST Quartz*. in *1975 Ultrasonics Symposium*. 1975.
28. Pohl, A., et al. *Monitoring the tire pressure at cars using passive SAW sensors*. in *Ultrasonics Symposium, 1997. Proceedings., 1997 IEEE*. 1997.
29. Wen, W., et al., *Optimal design on SAW sensor for wireless pressure measurement based on reflective delay line*. Vol. 139. 2007, Kidlington, ROYAUME-UNI: Elsevier. 5.
30. *U.S. Patent No. 5,585,571*.
31. Łepkowski, S.P.M., J. A.; Jurczak</Font>, G., *Nonlinear Elasticity in Wurtzite GaN/AlN Planar Superlattices and Quantum Dots.* Acta Physica Polonica A, 2006. **108**(11): p. 749.
32. Lucklum, R. and P. Hauptmann, *The quartz crystal microbalance: mass sensitivity, viscoelasticity and acoustic amplification.* Sensors and Actuators B: Chemical, 2000. **70**(1–3): p. 30-36.

33. ZHANG, H. and E.S. KIM, *Micromachined acoustic resonant mass sensor*. Vol. 14. 2005, New York, NY, ETATS-UNIS: Institute of Electrical and Electronics Engineers. 8.
34. Wingqvist, G., V. Yantchev, and I. Katardjiev, *Mass sensitivity of multilayer thin film resonant BAW sensors.* Sensors and Actuators A: Physical, 2008. **148**(1): p. 88-95.
35. Roshan, K., R.D.S. Yadava, and R.P. Tandon, *Mass sensitivity analysis and designing of surface acoustic wave resonators for chemical sensors.* Measurement Science and Technology, 2009. **20**(5): p. 055201.
36. Gabrielson, T.B., *Mechanical-thermal noise in micromachined acoustic and vibration sensors.* Electron Devices, IEEE Transactions on, 1993. **40**(5): p. 903-909.
37. Cleland, A.N. and M.L. Roukes, *Noise processes in nanomechanical resonators.* Journal of Applied Physics, 2002. **92**(5): p. 2758-2769.
38. Gagnepain, J.J., et al. *Relation Between 1/f Noise and Q-Factor in Quartz Resonators at Room and Low Temperatures, First Theoretical Interpretation*. in *Thirty Fifth Annual Frequency Control Symposium. 1981*. 1981.
39. Driscoll, M.M. and W.P. Hanson. *Measured vs. volume model-predicted flicker-of-frequency instability in VHF quartz crystal resonators*. in *Frequency Control Symposium, 1993. 47th., Proceedings of the 1993 IEEE International*. 1993.
40. Kaajakari, V., *Practical MEMS*. 2009, Las Vegas, Nev.: Small Gear Pub. xvi, 465 p.
41. *IEEE Standard Definitions of Physical Quantities for Fundamental Frequency and Time Metrology - Random Instabilities.* IEEE Std 1139-1999, 1999: p. 0_1.
42. Vig, J.R. and F.L. Walls. *A review of sensor sensitivity and stability*. in *Frequency Control Symposium and Exhibition, 2000. Proceedings of the 2000 IEEE/EIA International*. 2000.
43. Walls, F.L. and J.R. Vig, *Fundamental limits on the frequency stabilities of crystal oscillators.* Ultrasonics, Ferroelectrics and Frequency Control, IEEE Transactions on, 1995. **42**(4): p. 576-589.
44. Bjurstrom, J., G. Wingqvist, and I. Katardjiev, *Synthesis of textured thin piezoelectric AlN films with a nonzero C-axis mean tilt for the fabrication of shear mode resonators.* Ultrasonics, Ferroelectrics and Frequency Control, IEEE Transactions on, 2006. **53**(11): p. 2095-2100.
45. Electrical, I.o., et al., *The IEEE standard dictionary of electrical and electronics terms*. 1997: Institute of Electrical and Electronics Engineers.
46. Parker, T.E. *Characteristics and Sources of Phase Noise in Stable Oscillators*. in *41st Annual Symposium on Frequency Control. 1987*. 1987.

Acta Universitatis Upsaliensis

Digital Comprehensive Summaries of Uppsala Dissertations from the Faculty of Science and Technology 933

Editor: The Dean of the Faculty of Science and Technology

A doctoral dissertation from the Faculty of Science and Technology, Uppsala University, is usually a summary of a number of papers. A few copies of the complete dissertation are kept at major Swedish research libraries, while the summary alone is distributed internationally through the series Digital Comprehensive Summaries of Uppsala Dissertations from the Faculty of Science and Technology.

Distribution: publications.uu.se
urn:nbn:se:uu:diva-173182

ACTA
UNIVERSITATIS
UPSALIENSIS
UPPSALA
2012